Durao, D., and J. H. Whitelaw, "Turbulent Mixing in the Developing Region of Coaxial Jets," *J. Fluid Eng.*, 95, 467 (1973).
Fejer, A. A., T. P. Torda, L. Boehman, K. N. Ghia, and W. G. Herman, "Research on Mixing of Coaxial Streams," *ARL 67-0058*, Ill. Inst. Technol., Chicago (Mar., 1967).
Harsha, P. T., "Free Turbulent Mixing: A Critical Evaluation of Theory and Experiments," *Rept. AEDC-TR-71-36*, Aero. Ind., Arnold A. F. Station, Tenn. (Feb., 1971).
Hedman, P. O., and L. D. Smoot, "Particle-Gas Dispersion Effects in Confined Coaxial Jets," *AIChE J.*, 21, 372 (1975).
Memmott, V. J., "Rates of Mixing of Particles and Gases in Confined Jets," M.S. thesis, Brigham Young Univ., Provo, Utah (Apr., 1977).
Skinner, F. D., R. W. Hanks, and L. D. Smoot, "A Facility for Study of Turbulent Mixing and Kinetic Processes in an Entrained Coal Gasifier," Paper No. 7655, Western States Section/Combustion Institute, La Jolla, Calif. (Fall, 1976).
Smoot, L. D., "Turbulent Mixing Coefficients for Compressible Coaxial Submerged and Coflowing Jets," *AIAA J.*, 14, 1699 (1976).
———, and L. D. Allred, "Particle and Gas Mixing Effects in Confined Nonparallel Coaxial Jets," *ibid.*, 13, 721 (1975).
Smoot, L. D., and L. A. Fort, "Confined Jet Mixing with Nonparallel Multiple-Port Injection," *ibid.*, 14, 419 (1976).
Smoot, L. D., and W. E. Purcell, "Model for Mixing of a Compressible Free Jet with a Moving Environment," *ibid.*, 5, 2044 (1967).
Stowell, D. E., and L. D. Smoot, "Turbulent Mixing Correlations in Free and Confined Jets," AIAA Paper No. 73-1194, AIAA/SAE 9th Propulsion Conference, Las Vegas, Nev. Nov. 5-7, 1973).
Thurgood, J. R., L. D. Smoot, and D. Rees, "A Facility to Study the Effects of Turbulent Mixing in Pulverized Coal Combustion," Paper No. 76-54, Western States Section/Combustion Institute, La Jolla, Calif. (Fall, 1976).
Tufts, L. W., and L. D. Smoot, "A Turbulent Mixing Coefficient Correlation for Coaxial Jets with and Without Secondary Flows," *J. Spacecraft Rockets*, 8, 1183 (1971).

Manuscript received June 17, 1977; revision received December 23, and accepted January 5, 1978.

Dispersion Measurement in Clogged Filter Beds: A Diagnostic Study on the Morphology of Particle Deposits

HEMANT PENDSE
CHI TIEN
R. RAJAGOPALAN
and
R. M. TURIAN

Department of Chemical Engineering and Materials Science
Syracuse University
Syracuse, New York 13210

The use of tracer dispersion measurements in conjunction with associated pressure drop data, as an indirect diagnostic technique for the determination of particle deposit morphology in deep-bed filters, was investigated. The dispersion measurements consisted of the injection of an electrolyte tracer pulse at the inlet and the monitoring of the tracer peak as it traveled down the bed, while the pressure drop data consisted of the axial pressure gradient histories as deposition took place. These data are interpreted using dispersion and pressure drop theories established on the basis of assumed models of deposit morphology. The validity of this technique was confirmed experimentally.

SCOPE

The development of an experimental procedure for the determination of the morphology of particle deposits in a clogged filter bed using a combination of tracer dispersion and pressure drop measurements is examined. In concession to the inherent difficulties associated with possible direct methods of ascertaining the nature of the deposited material in a practical filter bed, the method explored here is indirect and essentially inferential. The basic idea of the present diagnostic procedure is to develop pressure drop expressions corresponding to various assumed deposit morphologies. Thus, a quantitative description of the change of the bed structure in the clogged filter can be obtained from values of the pressure drop increase. Further, using the inferred data on the altered bed structure, calculations relating to the response of a tracer pulse injected at the bed inlet, and in particular those relating to the speed of travel of the tracer peak through the bed, are carried out. These calculated predictions are then compared with experimental tracer dispersion measurements. Poor agreement between prediction and experiment would mean that the original assumed deposit morphology is inappropriate, while satisfactory agreement would at least suggest that the basic model assumed for the distribution of deposited matter is plausible and a suitable candidate for further development. The work reported here consists of three parts: the analysis of the convective dispersion problem relating to the response of a tracer pulse injected into a clogged filter bed, the development of relationships between pressure drop increase and change in bed structure due to clogging corresponding to assumed deposit morphologies, and dispersion measurement in a clogged test filter resulting from the filtration of aqueous talc suspensions in order to confirm the validity of the technique.

R. Rajagopalan is with the Department of Chemical and Environmental Engineering, Rensselaer Polytechnic Institute, Troy, New York 12181.

0001-1541-78-9495-0473-$01.55.

CONCLUSIONS AND SIGNIFICANCE

The principal objective of this research is to develop a feasible, relatively noninterfering method for determining the deposit morphology in a clogged filter bed. The research is particularly relevant to deep-bed filter operation since the amount, and especially the distribution within the bed, of deposited matter has a profound effect upon the dynamic behavior of the filter and, of course, is decisive with respect to the pressure drop increase. The present calculations confirm that tracer dispersion effects in a clogged filter are sufficiently sensitive to the nature of the assumed deposit morphology to form the basis of an adequately discriminating diagnostic technique. Comparison between theoretical and experimental tracer dispersion results obtained from a test filter clogged with talc powder yields conclusions consistent with earlier observations based on two-dimensional model filters and therefore adds credence to the utility of the technique.

The prediction of the response of a filter bed to the structural changes in its pore geometry caused by particle deposition has been a source of great difficulty in the understanding of deep-bed filtration. Considerable advances have been made in recent years in modeling the retention efficiency and the pressure drop characteristics of a clean filter (Payatakes, Tien and Turian, 1974*a, b;* Rajagopalan and Tien, 1976), yet the major portion of the filtration occurs in a bed whose porous structure is continuously altered. That the effectiveness of a filter and the pressure drops across the filter are significantly sensitive to the exact nature of these alterations is amply demonstrated in the literature (Herzig, Leclere, and LaGoff, 1970; Heertjes, 1957). Particularly illustrative of these is the ingenious series of experiments reported by Maroudas and Eisenklam (1965) which were performed with the use of a specially designed two-dimensional filter. Maroudas and Eisenklam observed that even with the same filter bed and the same type of particle, differences in flow rate and particle size may lead to three different results: gradual constriction of all junctions, leading to nonretention; blocking of some junctions, leading to nonretention; and blocking of some junctions, leading to complete blocking of the bed and subsequently to cake filtration. Other properties of the suspension may also exert significant influence in this regard. For example, Stein (1940) observed, in the filtration of ferric floc, the formation of relatively smooth coating over the cylindrical rods which constitute the filter media, while a pattern of nonuniform but smooth coating extending only over the upstream portion of the grain was found in the case of calcium carbonate suspensions by Cleasby and Bauman (1962) and for kaolinite particles by Ison and Ives (1969). Complications such as reentrainment, avalanching, dendritic deposition, breakage of deposited aggregates, and subsequent redeposition have also been observed in various experiments (Yao, 1968; Yao, Habibian and O'Melia, 1971; Ives, 1972; Leers, 1957).

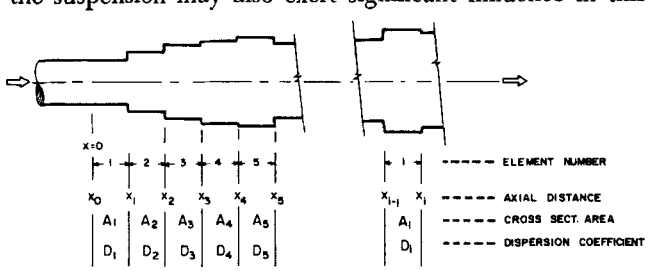

Fig. 1. A channel with step changes in cross-sectional area and dispersion coefficient.

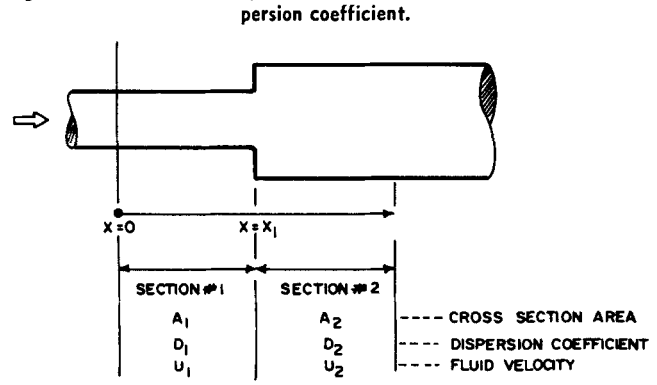

Fig. 2. A channel with a single step change in cross-sectional area and dispersion coefficient.

The above experimental information is available only in the form of some scattered observation (with the notable exception of Maroudas and Eisenklam, 1965); yet it sufficiently demonstrates the need to understand the dynamics of the structural changes in the filter as filtration progresses and the importance of the deposit morphology. Such information, however, has been difficult to obtain because of the inherent nature of the filtration system.

The purpose of this work is to develop a conceptually simple technique based on dispersion of tracers in porous media that is potentially useful in deducing structural changes in a filter as filtration proceeds. Firstly, the technique requires the development of equations to describe the dispersion of a pulse input along the axis of the bed (particularly, an equation for the rate of travel of the peak of concentration distribution), and this forms the first segment of the paper. Secondly, a geometric characterization of the morphology of the deposit is needed. This is presented in the second part of the paper and makes it possible to describe the structural change of a clogged filter bed in terms of the pressure drop increase data. Lastly, details of an experimental study to test the usefulness of the approach are presented.

It should be mentioned that the use of the dispersion measurement in the study of deep-bed filtration has been considered by previous investigators. Mints and Meltser (1970) conducted dispersion measurements in clogged filter beds similar to that performed in this paper and attempted to relate the rate of travel of tracer pulse through the bed with the porosity of the clogged bed. However, they failed to realize that such relationships cannot be derived without knowledge of deposit morphology, and the difference in dispersion between a clogged bed and a clean bed is not only due to the difference in porosity. Similar study currently is underway elsewhere (Ives, 1974). The idea of combining the dispersion measurements and pressure drop data to yield information concerning the deposit morphology as presented in this work has not, to the authors' knowledge, been attempted before.

DISPERSION IN A CLOGGED FILTER

The most significant feature required of a dispersion model of the clogged filter is that such a model should be capable of depicting, with sufficient accuracy and manageable ease, the variation of local cross-sectional areas available for flow (or local effective porosity) and dispersion coefficients as functions of spatial coordinates. Such variations would subsequently determine other parameters like interstitial velocities. In principle, these variations occur along all the three coordinates, since it is plausible to assume that the effect of deposition is to alter different regions differently. However, for reasons of simplification it is reasonable to consider that the major variation takes place along the axial direction. Accordingly, a clogged filter bed can be divided into numerous elements along the axis, each of which is sufficiently small to be considered homogeneous. Then to each element one can assign average values for cross-sectional areas, etc., as follows:

$$A_i = \frac{1}{\Delta x}\int_{x_{i-1}}^{x_i} A(x)dx \tag{1}$$

Thus, the variations in these properties from one element to the next represent collectively the structural changes in the bed along the axis. It will be shown in later sections of the paper how values may be assigned to these variables at any given element from pressure drop data with the use of a suitably selected porous media model and an assumed deposit morphology.

Solution of the Convective-Dispersion Equations

In order to solve the corresponding convective-dispersion equation, consider a cylindrical tube as shown in Figure 1 which undergoes step changes in cross-sectional area and other pertinent properties along the axial distance, which gives a model representation of a clogged bed. The problem then reduces to one of dispersion in a channel with step changes in geometry, grain size, and dispersion coefficient.

To obtain the solution for such a system, consider the simpler case of a channel with a single step change as shown in Figure 2, for which the governing equations can be stated as

$$\frac{\partial c}{\partial t} + u_1\frac{\partial c}{\partial x} = D_1\frac{\partial^2 c}{\partial x^2}; \quad 0 \leq x \leq x_1 \tag{2}$$

$$\frac{\partial c}{\partial t} + u_2\frac{\partial c}{\partial x} = D_2\frac{\partial^2 c}{\partial x^2}; \quad x_1 \leq x \tag{3}$$

with the corresponding initial and boundary conditions

$$c(x, 0) = 0 \qquad \text{for} \quad x > 0 \tag{4}$$

$$c(0, t) = (qA_1)\,\delta(t) \qquad \text{for} \quad t > 0 \tag{5}$$

In Equation (5), q is the mass of the tracer injected per unit cross-sectional area at the point of injection, $x = 0$. For the purpose of this work, one is interested in the time $t_m(x)$ at which the concentration peak reaches a particular distance x into the bed.

For $x \leq x_1$, the solution of Equation (2) with the given boundary conditions is given by

$$c(x, t) = \frac{q}{2\sqrt{\pi D_1 t}}\exp\left[-\frac{(x - u_1 t)^2}{4D_1 t}\right] \tag{6}$$

and the time of travel of the peak to the point x is

$$t_m(x) = \frac{x}{u_1}\left[\sqrt{\left(\frac{D_1}{u_1 x}\right)^2 + 1} - \left(\frac{D_1}{u_1 x}\right)\right] \tag{7}$$

For $x > x_1$, a translation of the axial variable will render Equation (3) in the following form

$$\frac{\partial c}{\partial t} + u_2\frac{\partial c}{\partial y} = D_2\frac{\partial^2 c}{\partial y^2}; \quad y = x - x_1,\ y \geq 0 \tag{8}$$

with the following conditions:

$$c(y, 0) = 0 \quad \text{for} \quad y > 0 \tag{9}$$

and

$$c(0, t) = \frac{q}{2\sqrt{\pi D_1 t}}\exp\left[-\frac{(x_1 - u_1 t)^2}{4D_1 t}\right] \tag{10}$$

The initial condition of Equation (9) is a consequence of Equation (4). The boundary condition at $y = 0$ follows from the fact that conservation equations for the tracer and the carrying fluid at the plane $y = 0$ demand

$$u_1 A_1 c(y, t)|_{0-} = u_2 A_2 c(y, t)|_{0+} \tag{11}$$

and

$$u_1 A_1 = u_2 A_2 \tag{12}$$

Consequently

$$c(y, t)|_{0-} = c(y, t)|_{0+} = c(0, t) = c(x, t)|_{x=x_1} \tag{13}$$

To solve the Equations (8) to (10), assume that $c(y, t)$ can be expressed by

$$c(y, t) = g(y, t)\exp\left[\frac{u_2 y}{2D_2} - \frac{u_2^2 t}{4D_2}\right] \tag{14}$$

Under this transformation, Equations (8) to (10) become

$$\frac{\partial g}{\partial t} = D_2\frac{\partial^2 g}{\partial y^2} \quad \text{for} \quad y \geq 0 \tag{15}$$

$$g(y, 0) = 0 \quad \text{for} \quad y > 0 \tag{16}$$

$$g(0, t) = \frac{q}{2\sqrt{\pi D_1 t}}\exp\left[-\frac{(x_1 - u_1 t)^2}{4D_1 t} + \frac{u_2^2 t}{4D_2}\right] = C_o(t)\exp\left(\frac{u_2^2 t}{4D_2}\right) \tag{17}$$

The solution of Equations (15) to (17) can be found from the application of Duhamel's principle and is given by

$$g(y, t) = \frac{y}{2}\frac{1}{\pi D_2}\int_o^t C_o(\tau)\exp\left[\frac{u_2^2\tau}{4D_2} - \frac{y^2}{4D_2(t - \tau)}\right]\frac{d\tau}{(t - \tau)^{3/2}} \tag{18}$$

Substitution of Equation (18) in (14) results in

$$c(x, t) = \frac{(x - x_1)}{2\pi D_2}\exp\left[\frac{u_2(x - x_1)}{2D_2} - \frac{u_2^2 t}{4D_2}\right] \cdot \int_o^t \frac{q}{2\sqrt{\pi D_1}}\exp\left[-\frac{(x_1 - u_1\tau)^2}{4D_1\tau} + \frac{u_2^2\tau}{4D_2} - \frac{(x - x_1)^2}{4D_2(t - \tau)}\right]\frac{d\tau}{(t - \tau)^{3/2}} \tag{19}$$

The time of travel of the peak to a point $x > x_1$ can be obtained numerically from the above expression for $c(x, t)$.

A generalization of the above procedure can be used for the solution for the case shown in Figure 1. First, denote the tracer concentration in the i^{th} element as

$$c_i(y_i, \tau_i) = c(x, t); \quad x_{i-1} < x \leq x_i \tag{20}$$

where

$$y_i = x - x_{i-1} \tag{21}$$

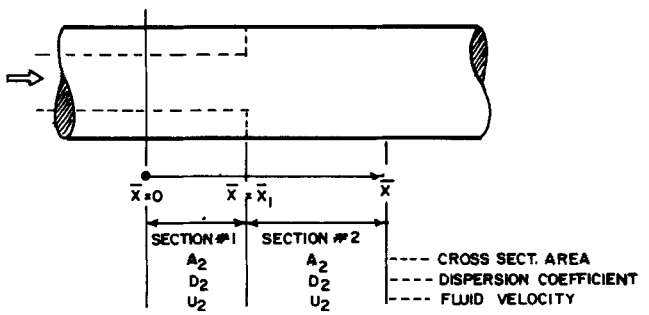

Fig. 3. An equivalent system corresponding to the channel with a single step change.

$$\tau_i = t \tag{22}$$

and

$$x_o = 0 \tag{23}$$

Then, the expressions for various elements are

$$c_1(y_1, \tau_1) = \alpha_1\beta_1\delta_1 \exp \gamma_1 \tag{24}$$

$$c_2(y_2, \tau_2) = \alpha_1\alpha_2 \int_o^{\tau_2} \tilde{\beta}_2\beta_1\delta_1\delta_2 \exp(\gamma_2 - \tilde{\gamma}_1)d\tau_1 \tag{25}$$

and in general

$$c_i(y_i, \tau_i) = \left[\prod_1^i \alpha_k\right] \int_0^{\tau_i} \int_0^{\tau_{i-1}} \cdots \int_0^{\tau_2} \beta_i \left[\prod_1^{i-1} \tilde{\beta}_k\right]\left[\prod_1^i \delta_k\right] \exp\left[\gamma_i + \sum_1^{i-1} \tilde{\gamma}_k\right] d\tau_{i-1} \ldots d\tau_1; \quad i \geq 2 \tag{26}$$

where

$$\alpha_k = \frac{1}{2\pi D_k}; \quad k = 1, 2, \ldots \tag{27}$$

$$\beta_1(y_1) = q \tag{28}$$

$$\beta_k(y_k) = y_k \exp\left[\frac{2u_k y_k \tau_k - u_k^2 \tau_k^2}{4D_k\tau_k}\right]; \quad k \geq 2 \tag{29}$$

$$\gamma_1(y_1) = -(y_1 - u_1\tau_1)^2/4D_1\tau_1 \tag{30}$$

$$\gamma_k(y_k) = \left[\frac{u_k^2\,\tau_{k-1}}{4D_k} - \frac{y_k^2}{4D_k(\tau_k - \tau_{k-1})}\right]; \quad k \geq 2 \tag{31}$$

$$\delta_1 = \tau_1^{-1/2} \tag{32}$$

$$\delta_k = (\tau_{k+1} - \tau_k)^{-3/2}; \quad k \geq 2 \tag{33}$$

$$\tilde{\beta}_k = \beta_k(y_k) \quad \text{at} \quad y_k = x_k - x_{k-1} \tag{34}^*$$

$$\tilde{\gamma}_k = \gamma_k(y_k) \quad \text{at} \quad y_k = x_k - x_{k-1} \tag{35}^*$$

Detailed derivations of the above expressions are presented elsewhere (Pendse, 1977).

It is obvious that very tedious calculations are required if the number of elements is large. For this reason, an approximate method is developed below.

Approximate Equations of t_m

For the tube with single step change shown in Figure 2, the time for the travel of the peak to any point $x \leq x_1$ is given by Equation (7). To obtain a similar expression for $x > x_1$, we shall assume that an equivalent system exists such that the first section of the tube can be replaced with one of given length which has the physical parameters of those of section two (that is, the same cross-sectional area A_2 and dispersion coefficient D_2; see Figure 3). It then follows that the time of travel of the tracer peak along the axial distance $\bar{x}$ in this equivalent system for a pulse input at $\bar{x} = 0$ is given by

$$t_{m,e}(\bar{x}) = \frac{\bar{x}}{u_2}\left[\sqrt{\left(\frac{D_2}{u_2\bar{x}}\right)^2 + 1} - \left(\frac{D_2}{u_2\bar{x}}\right)\right] \tag{36}$$

On physical grounds, the selection of this hypothetical section will be made in such a manner that the time required for the tracer peak to travel from $x = 0$ to $x = x_1$ in the actual system is the same as the time required by the peak in the equivalent system to move from $\bar{x} = 0$ to $\bar{x} = \bar{x}_1$; that is

$$t_m(x_1) = \frac{x_1}{u_1}\left[\sqrt{\left(\frac{D_1}{u_1x_1}\right)^2 + 1} - \left(\frac{D_1}{u_1x_1}\right)\right] \equiv t_{m,e}(\bar{x}_1) = \frac{\bar{x}_1}{u_2}\left[\sqrt{\left(\frac{D_2}{u_2\bar{x}_1}\right)^2 + 1} - \left(\frac{D_2}{u_2\bar{x}_1}\right)\right] \tag{37}$$

Clearly, Equation (37) is the defining equation for $\bar{x}_1$ and relates the equivalent system to the actual one in terms of their respective axial distances. This expression can be considerably simplified if the two Peclet numbers ($u_2\bar{x}_1/D_2$) and (u_1x_1/D_1) are much larger than unity. Under such conditions, the following approximation holds:

$$\bar{x}_1 = \frac{u_2}{u_1}x_1 + u_2\left[\frac{D_2}{u_2^2} - \frac{D_1}{u_1^2}\right] \tag{38}$$

For a given point $x > x_1$, the corresponding coordinate in the equivalent system $\bar{x}$ becomes

$$\bar{x} = x - x_1 + \bar{x}_1 \tag{39}$$

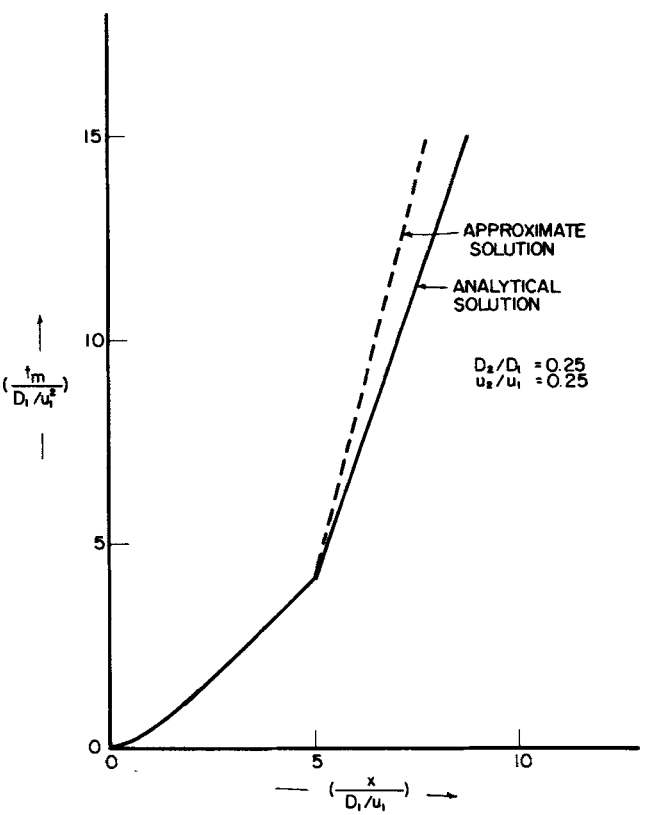

Fig. 4a. Calculated analytical and approximate solutions for time at peak arrival as a function of axial distance for $x_1/D_1/u_1 = 5.0$.

* $\tilde{\beta}_k$ and $\tilde{\gamma}_k$ are values of β_k and γ_k evaluated at the exit of the k^{th} element, respectively.

The equation for the time at which the concentration peak arrives at $x > x_1$ is then

$$t_m(x) = t_m(x_1) + t_{m,e}(\bar{x}) - t_{m,e}(\bar{x}_1) \qquad (40)$$

The value of $[t_m(x_1) - t_{m,e}(\bar{x}_1)]$ does not vanish as required by Equation (37), since the approximation given by Equation (38) is used in the transformation. In the above equation, the first term on the right-hand side is given by Equation (7) and the other two by Equation (36). With the repeated application of the above formulation, similar expressions for the peak travel time in a system consisting of any number of elements can be obtained. The time of arrival at the exit of the i^{th} element (that is, $x = x_i$) is given by

$$t_m(x_i) = t_m(x_{i-1}) + t_m^{(i)}(x_i - x_{i-1} + \bar{x}_{i-1}) - t_m^{(i)}(\bar{x}_{i-1}); \quad i \geq 1 \qquad (41)$$

where

$$\bar{x}_{i-1} = \left(\frac{u_i}{u_i - 1}\right)(\bar{x}_{i-2} + x_{i-1} - x_{i-2}) + u_i\left(\frac{D_i}{u_i^2} - \frac{D_{i-1}}{u_{i-1}^2}\right); \quad i \geq 2 \qquad (42)$$

$$\bar{x}_0 = 0 \qquad (43)$$

$$t_m^{(i)}(x) = \frac{x}{u_i}\left[\sqrt{\left(\frac{D_i}{u_i x}\right)^2 + 1} - \left(\frac{D_i}{u_i x}\right)\right]; \quad i \geq 1 \qquad (44)$$

and

$$t_m^{(1)}(\bar{x}_o) = t_m(x_o) = 0 \qquad (45)$$

It is evident that the above equations are much simpler to use than the analytical solutions. However, the derivation of the approximations rests on intuitive reasoning, and its accuracy cannot be assumed except through direct comparison. Figures 4*a* to 4*c* present such a comparison for various values of D_i's and u_i's for a bed consisting of two elements. It is obvious that the two expressions give essentially the same results for large values of the Peclet number x_1u_1/D_1. Similarly, the condition for the general expression [that is, Equation (4)] to be valid is that the Peclet numbers corresponding to the first $(i-1)$ sections x_1u_1/D_1, x_2u_2/D_2 .... $x_{i-1}, u_{i-1}/D_{i-1}$ should be sufficiently large. The Peclet number is directly proportional to the length of the segment. On the other hand, the representation of a clogged filter by a sequence of segments connected in series as shown in Figure 1 requires that the segment length should be kept sufficiently small so that the properties of each segment can be considered as constant. Thus, in order to utilize this approximate expression, the other parameters (that is, D_i and u_i) should be such as to allow the selection of a proper segment length which satisfies both of the requirements.

UNIT BED ELEMENT AND DEPOSIT MORPHOLOGY

The dispersion measurement by itself cannot provide information on the type of deposition in the filter. In order to infer the morphology of the deposit on the basis of the response of the clogged bed to a pulse of tracer, it is necessary first to assign an appropriate model to represent the unit bed element of the filter bed and second to use such an element in conjunction with various possible morphologies of deposit to predict the corresponding outcomes of the dispersion experiment. This procedure provides a series of possible outcomes against which the experimental observation can be compared.

The choice of the unit bed element will often rest on other considerations such as, for instance, its ability to predict the deposition rate based on trajectory calculations. Two models are used in the present study: a constricted

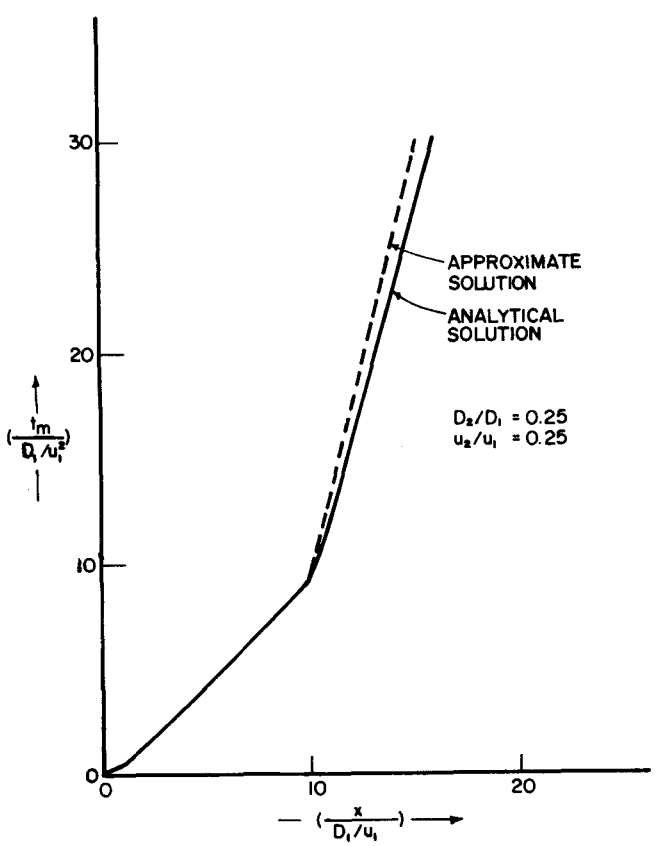

Fig. 4b. Calculated analytical and approximate solutions for time at peak arrival as a function of axial distance for $(x_1/D_1/u_1) = 10.0$.

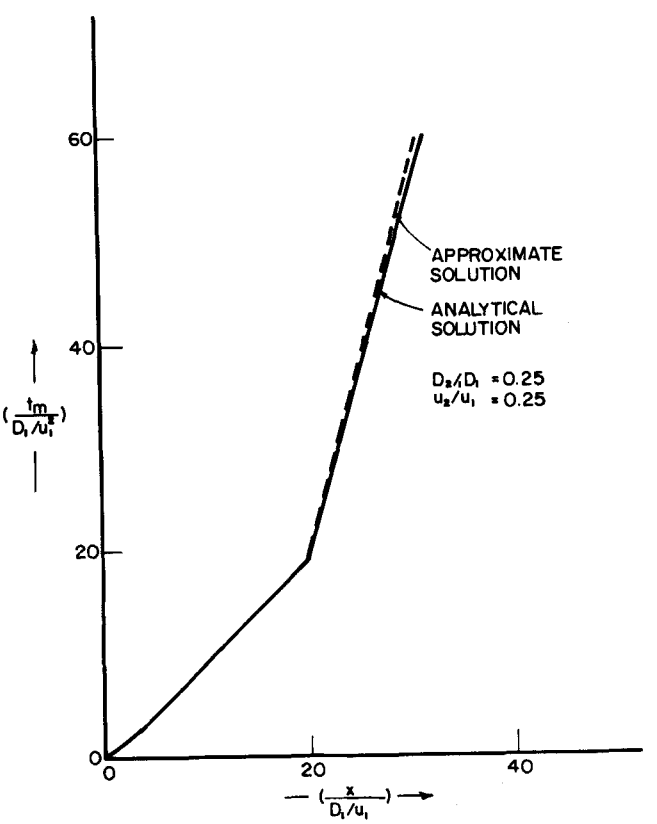

Fig. 4c. Calculated analytical and approximate solutions for time at peak arrival as a function of axial distance for $x_1/D_1/u_1 = 20.0$.

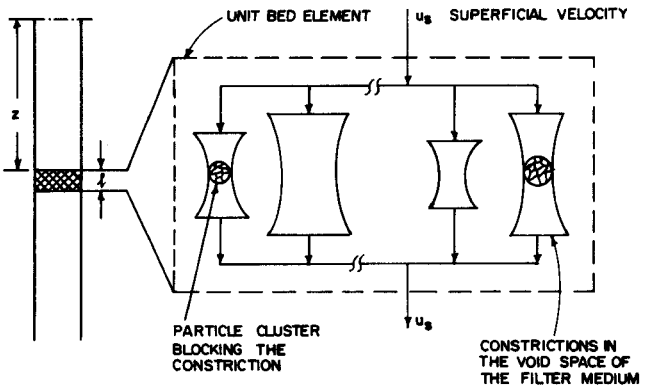

Fig. 5. Constriction blocking illustrated using the constricted tube model.

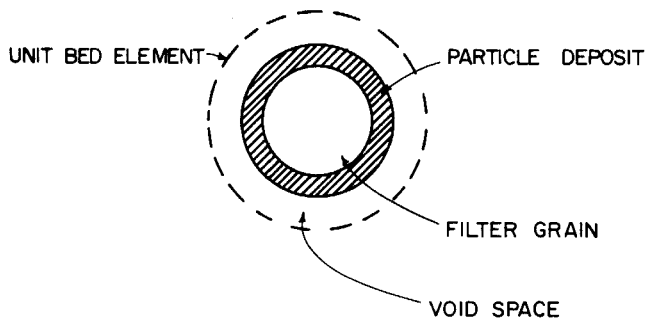

Fig. 6. Smooth coating in the case of the sphere-in-cell.

tube model for porous media advanced by Payatakes, Tien, and Turian (1974*a*, *b*) and a sphere-in-cell model described in Rajagopalan and Tien (1976). Figures 5 and 6 present simplified pictures of the above two porous media models. Thus, a filter bed may be considered to be an assembly of such unit bed elements connected in series.

The changes that occur in a unit bed element as deposition progresses can take many forms and may vary significantly from case to case. Further, it is extremely difficult, if not impossible, to provide an exact morphological description of the deposit. However, since the major intent of this paper is to provide an illustration of the use of the technique described earlier, we shall describe two limiting cases of the deposit morphology.

Constriction Blocking

As the suspension flows through the flow passages in the bed, one limiting condition that could develop is the complete blockage of some constrictions. This blocking mode of deposition has been visually documented by Maroudas and Eisenklam (1965) in their two-dimensional filters and has been proposed in explanation of their experimental observations on three-dimensional granular beds. The blockage of flow passages is a natural consequence if the suspended particles to be filtered have dimensions comparable to or greater than those of the pore constrictions in the filter medium. But this is not likely to occur, at least in a well-designed system, since particle removal by sieving is to be avoided. A more likely possibility is the recapture of large aggregates which are originally formed on the surface of the grains and dislodged and reentrained subsequently as recently proposed by Payatakes, Brown, and Tien (1977). An illustration of this mode of deposition is shown in Figure 5.

Smooth Deposition

On the other extreme is the case of smooth deposition on grain surfaces as observed by Stein (1940). This is sketched in Figure 6 for the sphere-in-cell model. This situation is likely to occur when the suspended particles are much smaller than the grains, and the shadow effect exhibited by the particles is not significant (see Tien, Wang, and Barot, 1977). A smooth coating on the grain surface tends to reduce the constriction diameter as well as to increase the effective grain size.

Effect of Deposition on Pressure Drop

For the estimation of the pressure drop across a filter bed, the packed bed is often viewed as a bundle of tangled tubes with complicated cross sections. It is convenient to define a mean hydraulic radius by

$$R_h = \epsilon/a_v(1-\epsilon) \tag{46}$$

For grains, a corresponding equivalent diameter may be defined as

$$D_g = 6/a_v \tag{47}$$

The Hagen-Poiseuille formula for pressure gradient in tubes gives

$$\frac{dp}{dz} = u\frac{2\mu}{R_h} \tag{48}$$

Combination of Equations (46) to (48) will result in an expression for the pressure gradient in terms of the equivalent grain diameter, porosity, and interstitial velocity. But a constant multiple of the resulting expression is often used because of its better correspondence to empirical observations and is known as the Blake-Kozeny equation:

$$\frac{dp}{dz} = \frac{150\mu}{D_g^2}u\left(\frac{1-\epsilon}{\epsilon}\right)^2 \tag{49}$$

Equation (49) holds good for $\epsilon < 0.5$ and $D_g\rho\, u_s/\mu(1-\epsilon) < 10$ (see Bird, Stewart, and Lightfoot, 1960; pp. 197-9). From Equation (49) it follows that the ratio of pressure gradients of the clogged and clean filter is given by

$$\frac{\left(\frac{dp}{dz}\right)}{\left(\frac{dp}{dz}\right)_o} = [\lambda(z)]^{-2}\left[\left(\frac{1}{r(z)}\right)\right]\left(\frac{\epsilon_0}{\epsilon}\right)^2\left(\frac{1-\epsilon}{1-\epsilon_o}\right)^2 \tag{50}$$

where

$$\lambda(z) = D_g/D_{g,o} \tag{51}$$

$$r(z) = u_o/u \tag{52}$$

The above expression shows that a complete description of the change of structure of the filter media due to bed clogging can not be made based on pressure drop data alone. However, if prior assumption is made concerning the deposit morphology, additional expressions relating the values of λ, r, and ϵ for a given degree of deposition can be developed. This additional relationship together with the expressions of Equation (50) make it possible to obtain the qualitative information about the structural change of a clogged filter bed which can be used for the prediction of the dispersion behavior.

Deposition Morphology—Blocking Mode. The blocking mode of deposition primarily results in the reduction of the number of flow passages, while the geometry and hence the hydraulic characteristics of the open passages remain the same as in clean bed (see Figure 5). Consequently, the increased velocity in the unclogged channels causes a corresponding increase in the pressure drop, while the mean hydraulic radius and equivalent grain diameter remain unchanged. The factor by which the pressure gradient increases can then be obtained directly from Equation (50):

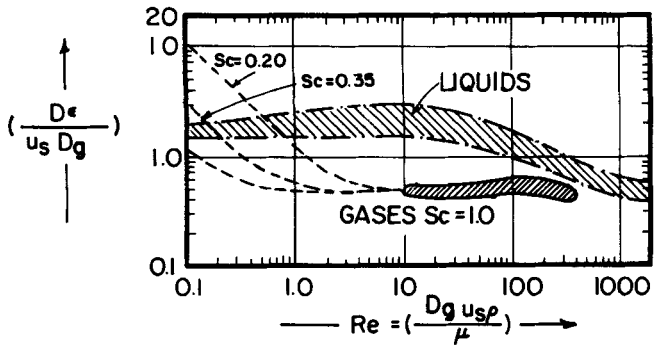

Fig. 7. Experimental findings on dispersion of fluid flow through packed bed. From *Chemical Reaction Engineering*, p. 282 (1977). Reproduced by permission of John Wiley & Sons.

$$\frac{(dp/dz)}{(dp/dz)_o} = \frac{1}{r(z)} \tag{53}$$

Deposition Morphology—Smooth Coating. On the contrary, the effect of smooth deposition is to decrease the available area and porosity and to increase the effective grain size all across the unit bed element. It can be shown in this case that

$$\frac{A}{A_o} = \frac{\epsilon}{\epsilon_o} = \frac{u_o}{u} = r(z) \tag{54}$$

This reduces Equation (50) to

$$\frac{(dp/dz)}{(dp/dz)_o} = \lambda^{-2} r^{-3} \left[\frac{1 - r\,\epsilon_o}{1 - \epsilon_o}\right]^2 \tag{55}$$

Furthermore, with the case of the sphere-in-cell model (see Figure 6) for the representation of the unit bed element, λ is given by

$$\lambda = [(1 - \epsilon)/(1 - \epsilon_0)]^{1/3} \tag{56}$$

One has for this model

$$\frac{(dp/dz)}{(dp/dz)_o} = r^{-3} \left[\frac{1 - r\,\epsilon_o}{1 - \epsilon_o}\right]^{4/3} \tag{57}$$

Estimation of Changes in the Dispersion Coefficient

Experimental findings on dispersion coefficients in packed beds as summarized by Bischoff (1961) indicate that the intensity of dispersion measured by (D/uD_g) remains approximately constant for Reynolds number $(D_g u_s \rho/\mu)$ ranging from 0.1 to 10 (see Figure 7). Thus, if the local Reynolds number stays within this range

$$\frac{D}{uD_g} = \frac{D_o}{u_o D_{g,o}} \tag{58}$$

Consequently

$$\frac{D}{D_o} = \frac{D_g}{D_{g,o}} \cdot \frac{u}{u_o} = \frac{\lambda(z)}{r(z)} \tag{59}$$

Equation (59) shows that the change in the dispersion coefficient from one element to the next along the axis z can be estimated if the changes in the grain diameter and interstitial velocity are known.

Application of the Dispersion Technique

The development presented above permits the prediction of the response of a clogged filter to a tracer pulse input at the inlet of the bed. From the pressure drop data,

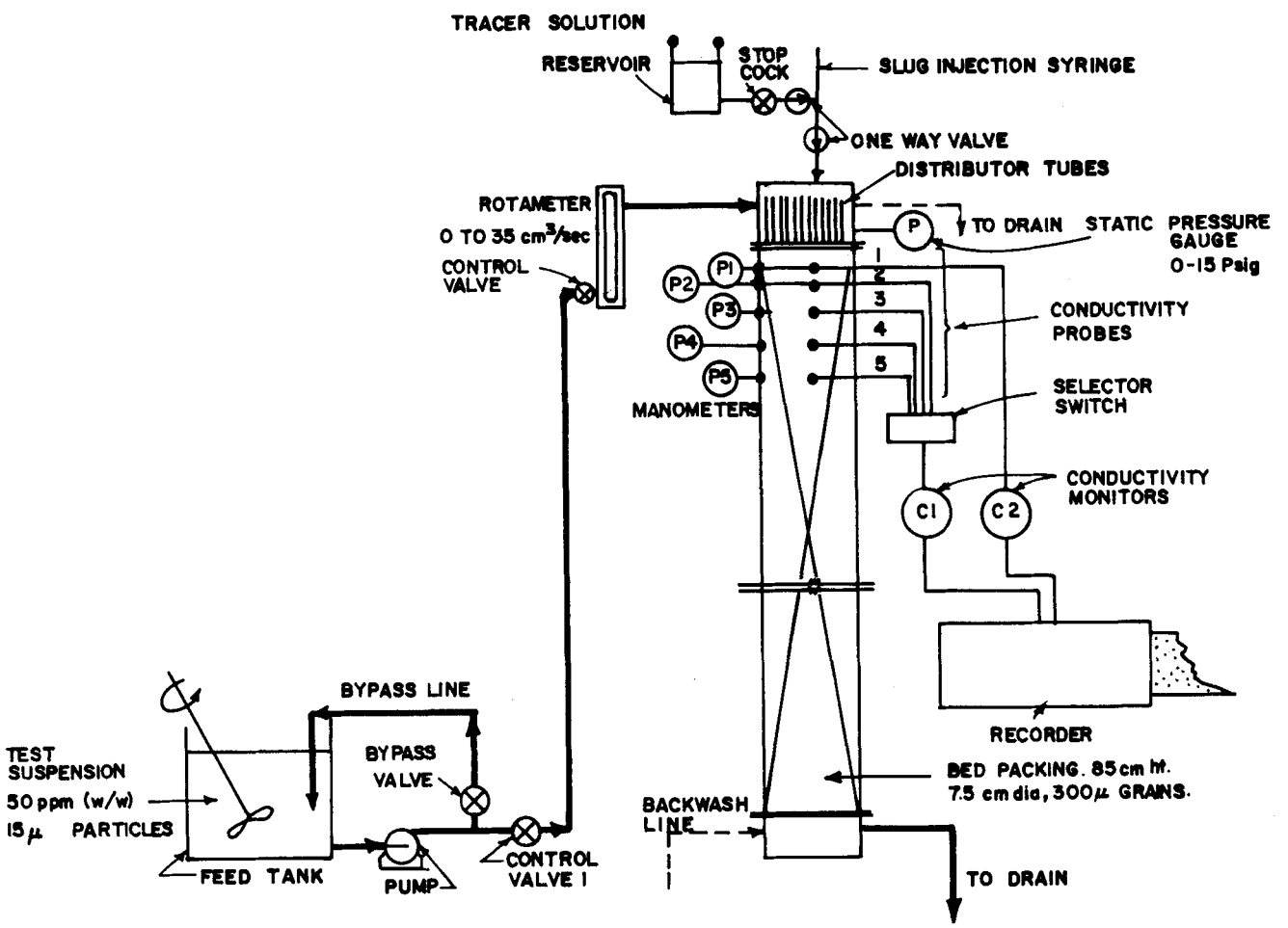

Fig. 8. A schematic diagram of the equipment set-up.

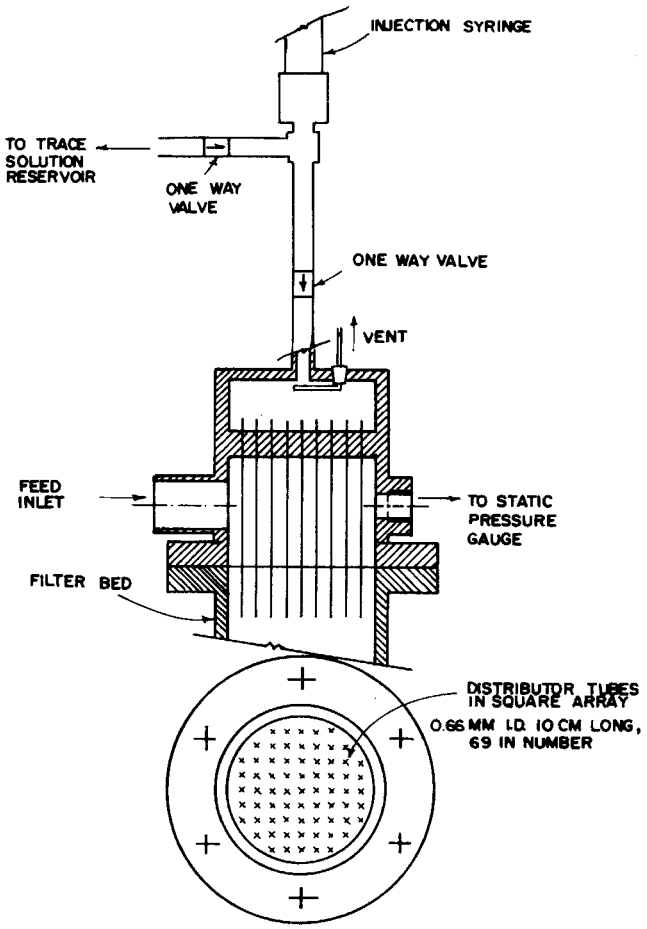

Fig. 9. Detailed diagram of the tracer distributor section.

appropriate values can be found for the various pertinent parameters (A_i, u_i, D_i) for each segment of the clogged filter. The time of travel of the tracer peak can be calculated from Equation (4) and compared with experimental measurements described in later sections.

EXPERIMENTAL STUDY

This section describes an experimental study that was conducted in order to illustrate the procedure of the diagnostic technique for morphology determination. The major part of experiment was concerned with the measurement of pressure drops and dispersion in a test filter at both clean and clogged states.

Experimental Apparatus

The major component of the apparatus (Figure 8) was the test filter made of a Plexiglas column of diameter 7.5 cm and length 85 cm and filled with 300 μm diameter glass beads. The filter was provided with five pressure taps and five conductivity probes at bed depths of 0, 1, 3, 6, and 9 cm. The conductivity probes were used for recording the tracer concentration on a strip chart recorder. The tracer injection unit, consisting of a tracer solution reservoir, an injection syringe, and a distributor assembly made up of sixty-nine thin stainless steel tubes, formed the head of the test filter (see Figure 9). During backwashing this was replaced by longer columns to provide room for bed expansion.

Experimental Procedure

Tap water at specific flow rates was used for measurements of pressure drops and dispersion in clean beds. Generally lower flow rates were used for the dispersion measurements. Since only two conductivity monitors were available, probe No. 1 (at the top of the bed) was permanently connected to one and served as the reference probe. The other probes were connected to the second monitor through a selector switch (see Figure 8). Thus, for any given injection of the tracer (0.1 N sodium chloride solution), a two-channel recorder was used to record the concentration histories at the reference probe and at any of the others.

Dispersion measurements in the clogged bed followed a similar procedure. Table 1 summarizes the experimental conditions.

At the end of each run, the filter was thoroughly backwashed with tap water for about 2 hr. The bed was then reconditioned by passing tap water, first at high flow rates (35 cm^3/s) for about half an hour and then at the desired flow rate until a constant pressure gradient was established.

Table 1. Filter-Bed Characteristics and Operating Conditions

(A) Filter-bed characteristic:

(a) Grain diameter	300 μm
(b) Particle diameter	15 μm
(c) Cross-sectional area	44.18 cm^2
(d) Height	85 cm
(e) Particle concentration in suspension	50 ppm (w/w)

(B) Operating conditions:

Run	Volumetric flow rate (cm^3/s)	Filtration time (hr)
A	21.8	2
B	21.8	2.5
C	21.8	3
D	21.8	3.5
E	14.3	2
F	18.0	1

Results

Table 2 presents a summary of the experimental runs conducted for this preliminary test. Figures 10 to 12 present the pressure drop and dispersion data for some typical runs. The pressure gradient reported in Table 2 for the clean bed is the average value of gradients from five identical runs, which differed from each other by about $\pm$ 5%. Figures 11 and 12 are composites of four successive dispersion measurements taken at one pair of probes at a time.

The dispersion measurements for the clean beds were used for the determination of D_o (the dispersion coefficient for the clean bed) with the procedure suggested by Bischoff and Levenspiel (1962). The corresponding pressure drop measurements were used to compute ϵ_o [with Equation (49)]. The calculated value of D_o is given in Table 3.

It was shown earlier that changes in the cross-sectional area, grain diameter, and dispersion coefficient can be computed from the increase in pressure drop as filtration proceeds. Using these, the time required for the concentration peak of the tracer (injected as a δ input at the inlet) can be calculated for comparison with experimental observations.

Application of this procedure is rather straightforward. The pressure gradient for the clean bed dH_o/dz and for the clogged bed dH/dz are first computed from figures similar to Figure 10. The gradient of the change in pressure drop $d(H - H_o)/dz$ can be obtained numerically as a function of z. From these, the ratio of pressure gradients $R(z)$ is obtained:

TABLE 2. EXPERIMENTAL DATA: RUN A

I. Pressure drop study						
(a) Volumetric flow rate	(cm^3/s)					21.8
(b) Superficial velocity	(cm/s)	u_s				0.49
(c) Reynolds number		$(D_g u_s \rho)/\mu$				1.47
(d) Filtration time	(hr)					2.0
I.A. Pressure drop-clean bed						
Bed depth, cm (z)	0	1	3	6	9	
Pressure drop, mm of Hg (H_0)	0	5	14	29	43	
Pressure drop gradient, mm of Hg/cm			4.8			
Bed voidage, ϵ_0			0.37			
I.B. Pressure drop—clogged bed						
Bed depth, cm (z)	0	1	3	6	9	
Pressure drop, mm of Hg (H)	0	12	23	41	59	
Head loss, mm of Hg ($H - H_0$)	0	7	9	12	16	
II. Dispersion measurements						
(a) Volumetric flow rate	(cm^3/s)					6.1
(b) Superfacial velocity	(cm/s)		u_s			0.14
(c) Interstitial velocity	(cm/s)		u			0.37
Bed depth, cm (z)	0	1	3	6	9	
Time required for peak travel s, ($t_{m,0}$) in clean bed	0	3	8	16	24	
Time required for peak travel in clogged bed s, (t_m)	0	1.5	5	12	19	
Ratio: ($t_m/t_{m,0}$)	0	0.5	0.625	0.75	0.79	

$$R(z) = \frac{(dp/dz)}{(dp/dz)_o} = \frac{(dH/dz)}{(dH/dz)_o} = 1 + \frac{d(H - H_o)/dz}{dH_o/dz} \tag{60}$$

The change in the interstitial velocity now follows from Equation (53) or (57) (depending on the assumed morphology). Using this, the change in dispersion coefficient can be computed and used for calculating the travel time of the peak from one probe to the next [Equations (41) to (45)].

For our calculations, we divided the first 9 cm of the bed into nine elements and applied the above procedure. (Elements beyond the top 9 cm were not considered, since they were not equipped with conductivity probes.) The computed and observed values of t_m were made dimensionless by dividing by $t_{m,o}$, the time of travel observed for the clean bed. Results for run A are presented as a function of z in Figure 13, and results of other runs are summarized in Table 4.

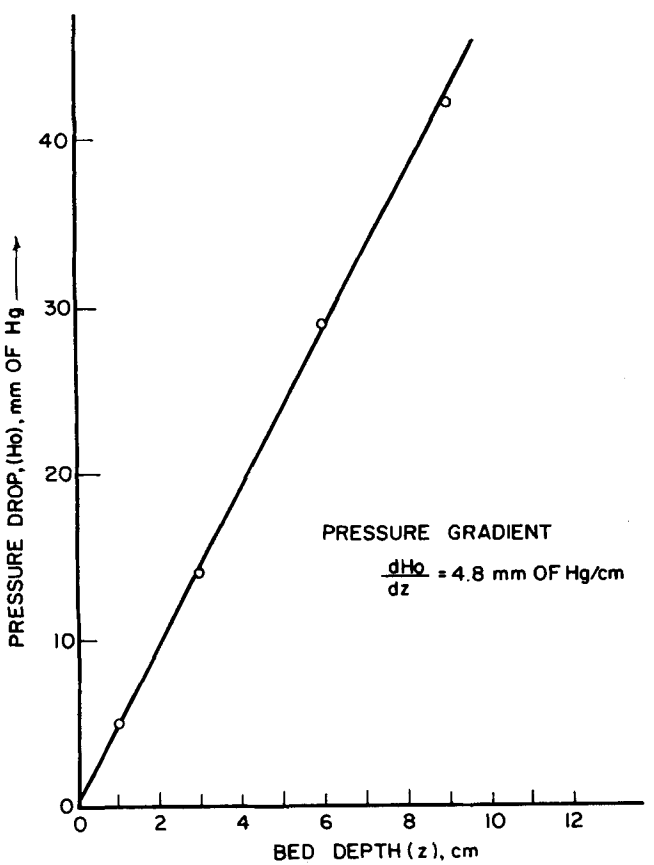

Fig. 10a. Pressure drop vs. bed depth for clean bed (run A).

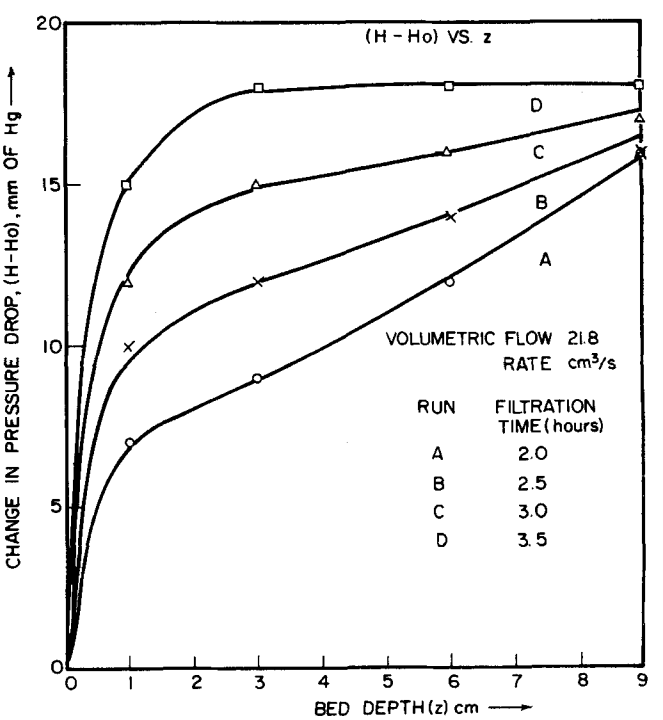

Fig. 10b. Change in pressure drop for clogged and clean test filter vs. bed depth for experimental runs A, B, C and D.

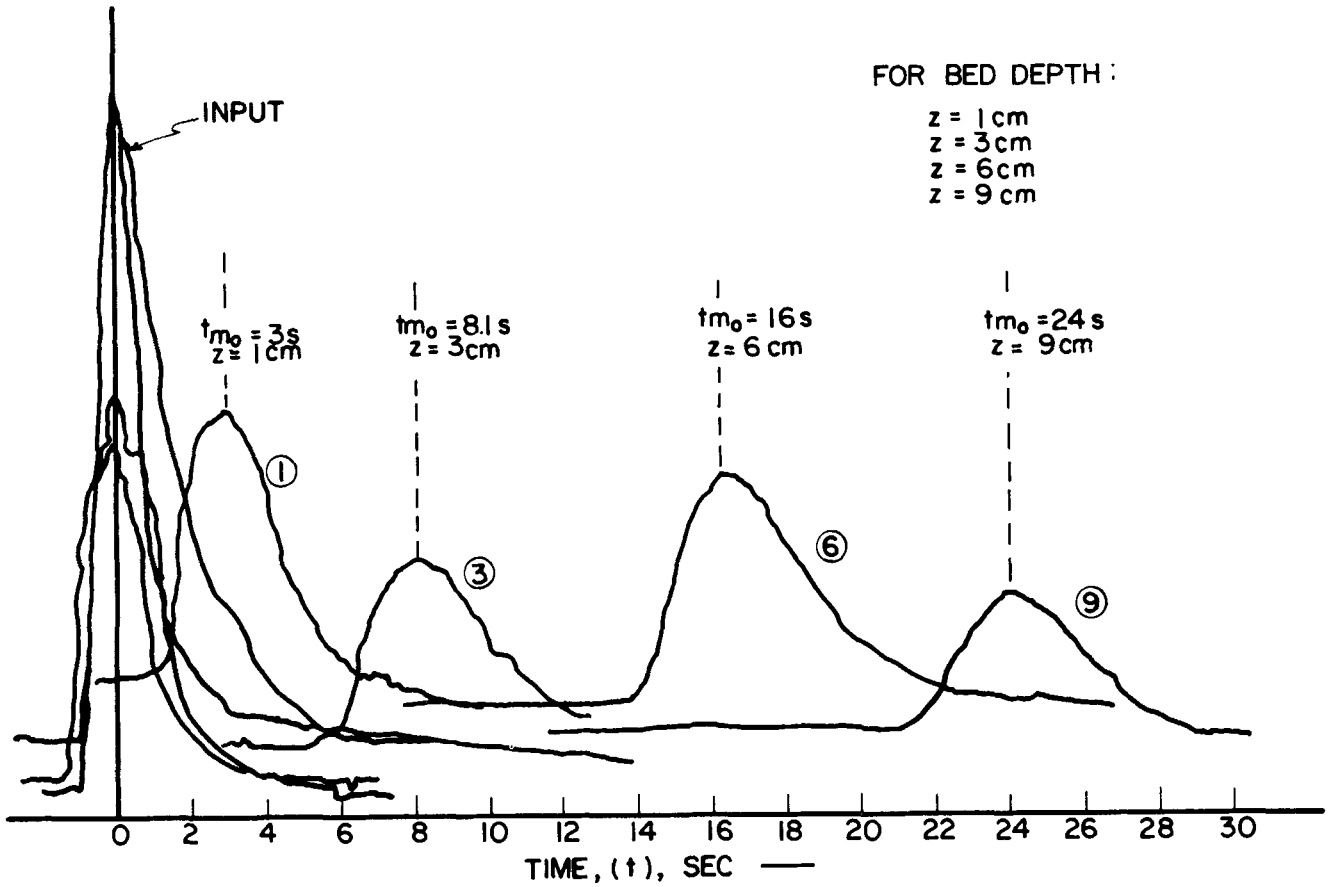

Fig. 11. Concentration vs. time response curves for A-input in a clean test filter.

TABLE 3. CALCULATION OF THE DISPERSION COEFFICIENT FOR THE CLEAN TEST FILTER

Bed voidage ϵ_0	0.395
Superfacial velocity u_s	0.31 cm/s
Interstitial velocity u_0	0.32 cm/s
Time constant (z/u_0)	
for $z = 6$ cm	18.75 s
for $z = 9$ cm	28.13 s
(a) For the concentration-time response curve at $z = 6$ cm	
$\Delta\sigma_t^2$	15.13 s^2
$\Delta\sigma^2$	0.043
(D_0/u_0z)	0.0199
D_0, dispersion coefficient 0.038 cm^2/s	
(b) For concentration-time response curve at $z = 9$ cm	
$\Delta\sigma_t^2$	20.83 s^2
$\Delta\sigma^2$	0.026
(D_0/u_0z)	0.0125
D_0, dispersion coefficient 0.036 cm^2/s	
Average value of dispersion coefficient	0.037 cm^2/s
Percent error	±2.5%

TABLE 4. COMPARISON BETWEEN PREDICTED AND MEASURED DISPERSION DATA

		Bed depth z, cm			
	$t_m/t_{m,o}$	1	3	6	9
Run A	Experimental	0.50	0.63	0.75	0.79
	Smooth coating	0.62	0.80	0.85	0.88
	Blocking mode	0.36	0.62	0.70	0.74
Run B	Experimental	0.45	0.67	0.77	0.83
	Smooth coating	0.70	0.84	0.90	0.93
	Blocking mode	0.24	0.55	0.70	0.78
Run C	Experimental	—	0.60	0.85	0.87
	Smooth coating	0.66	0.83	0.90	0.92
	Blocking mode	0.20	0.52	0.72	0.76
Run D	Experimental	—	—	0.86	0.94
	Smooth coating	0.65	0.83	0.91	0.94
	Blocking mode	0.18	0.55	0.74	0.81
Run E	Experimental	0.45	0.73	0.84	0.87
	Smooth coating	0.83	0.88	0.93	0.95
	Blocking mode	0.54	0.65	0.76	0.84
Run F	Experimental	0.33	0.63	0.76	0.83
	Smooth coating	0.62	0.81	0.90	0.93
	Blocking mode	0.19	0.51	0.71	0.82

DISCUSSION

The dispersion measurement results as summarized in Table 4 and shown in Figure 13 were found in general to be in good agreement with predictions based on assumptions that the deposit morphology is of the blocking mode. In this connection, it is worth noting that for the experimental work conducted in this study, the filter bed consisted of nearly uniform glass spheres of diameters of approximately 300 μm. In terms of the constricted tube, the average constriction of the filter bed is estimated to be about 60 to 70 μm. The suspended particles used to clog the test filter were angular with a mean diameter of 15 to 18 μm. Thus, the ratio of the particle size to constriction is roughly between one-fourth to one-third.

Maroudas and Eisenklam (1965) observed from their work on a two-dimensional filter that the deposition of angular particles was dominated by blocking mode for particle diameter, constriction diameter ratios between one-eighth and one-third. In fact, this seemed to be true in the

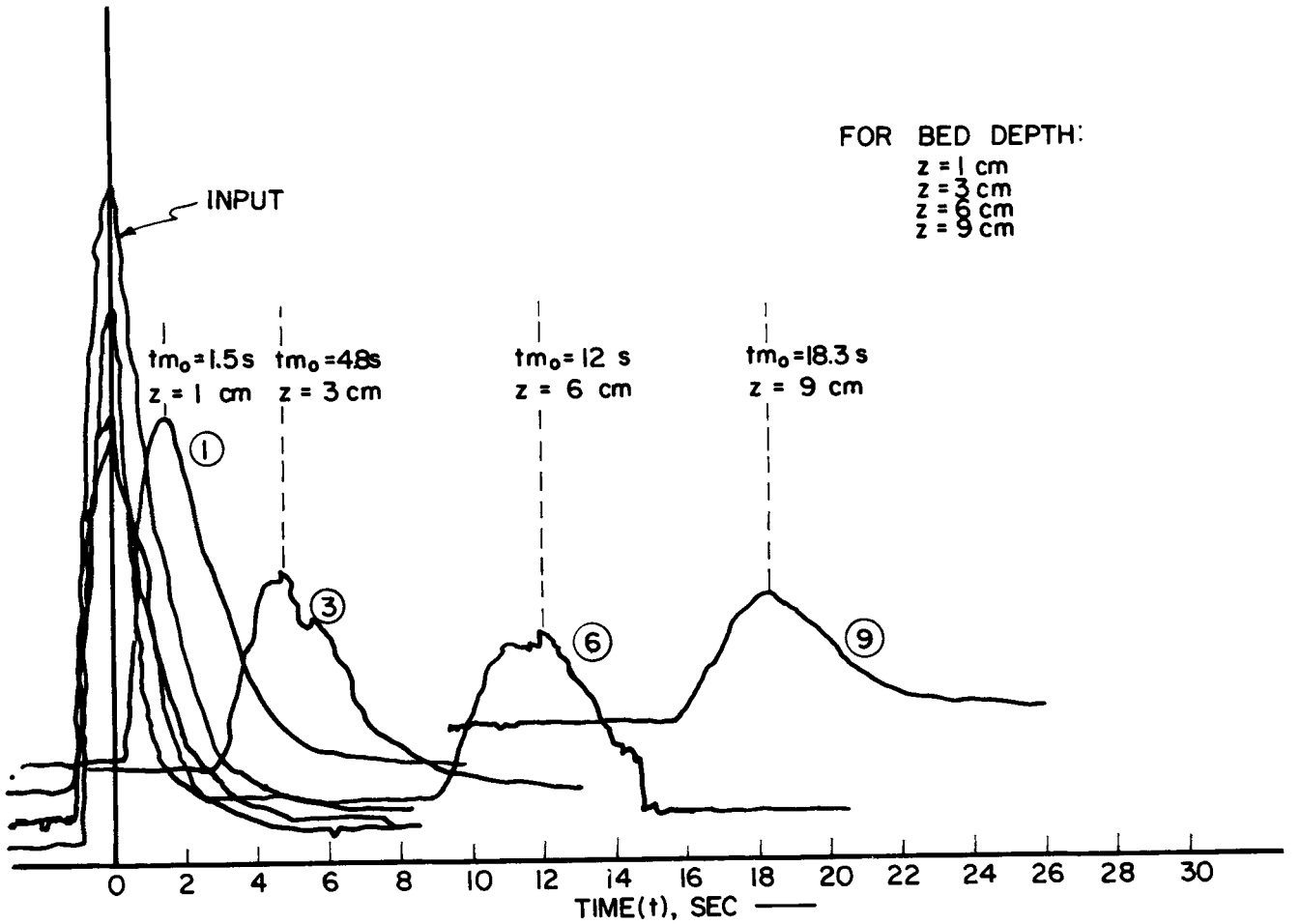

Fig. 12. Concentration vs. time response curves for a ∂-input in a clogged test filter.

case of their experiments with three-dimensional granular beds as well. The agreement between the conclusions based on dispersion measurement and the earlier work of Maroudas and Eisenklam therefore lends credence to the utility of the diagnostic teachings based on dispersion measurements. This conclusion was further reinforced by the fact that prior to the experiments reported in this paper, a series of trial experiments had been conducted in order to choose an appropriate set of conditions. Trial runs, in which glass beads of diameter 500 μm or over were used, resulted in very small pressure drop increases even after 10 hr or more of filtration using 15 μm diameter talc suspension. Further, in these cases deposition was seen to occur all across the depth over the top 10 to 15 cm as observed from the slight yellowish color of the grains (which very gradually changed to its natural murky white about 10 to 15 cm from the top). Dispersion measurements in these cases indicated that the travel times for the concentration peak changed almost imperceptibly from those for clean beds (indicating that retention was little and uniform). On the other hand, trial runs in which glass beads of about 200 μm were used resulted in a visibly thick, yellowish cake at the top of the bed with an accompanying pressure drop increase.

In the series of runs reported here, no visible cake appeared at the top surface, but a distinct color change along

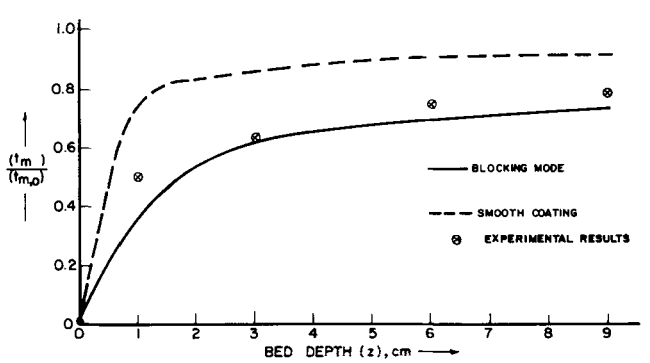

Fig. 13. Comparison between predicted and measured dispersion data (t_m vs a) for run A.

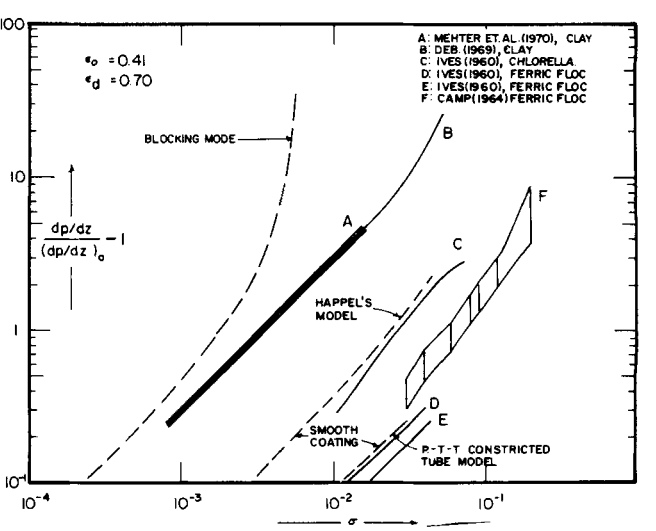

Fig. 14. Comparison between experimental and calculated values of pressure drop increase vs. specific deposit.

the depth was apparent. As filtration progressed, the shade darkened, indicating further deposition. The results presented in Figure 13 and Table 4 confirm the above observation in terms of $t_m/t_{m,o}$. Although the assumption of blocking mode as the dominant mode seems to underestimate the time of travel, the experimental results are sufficiently close. On the other hand, assumption of smooth coating results in significantly higher estimates for t_m.

To put the results in better perspective, the increases in pressure gradient due to particle deposition observed by various investigators are presented in Figure 14 as function of σ. This figure is taken from the earlier work of Payatakes, Brown, and Tien (1977) with corrections of certain apparent errors. The figure also shows the predictions based on blocking mode of deposition and smooth deposition. The former was originally calculated by Payatakes and Tien (1974) but is based on essentially the same procedure as presented in this paper. Two significant observations can be made regarding the results presented in this figure: The blocking mode does overestimate the results significantly at times, and, more importantly, experimental data show a very wide scatter, and no single mode of deposition can be relied on consistently.

The latter observation underscores the importance of the establishment of criteria which can be used to determine a priori the deposit morphology from a given set of system and operating parameters. In carrying out studies toward such a goal, experimental confirmation of the deposit morphology is obviously required. The technique established in this study is believed to fulfill such a requirement.

ACKNOWLEDGMENT

This work was performed under Grant Nos. GK-33976 and ENG 76-08755, National Science Foundation. The apparatus used in the experiments was built by R. S. Fleisher.

NOTATION

A = available cross-sectional area for fluid flow, cm^2
A_i = cross-sectional area available for flow at i^{th} element
a_v = specific wetted surface area of a filter grain (wetted surface/grain volume), cm^{-1}
c = tracer concentration, amount of tracer per unit volume of suspension, g/cm^3
D = dispersion coefficient, cm^2/s
D_g = equivalent grain diameter, cm
dH/dz = pressure gradient, mm of Hg/cm
dp/dz = pressure gradient, dynes/cm^2·cm
H = head loss at given bed depth, mm of Hg
q = quantity of tracer injected per unit available cross-sectional area g/cm^2
R = ratio of pressure gradient at a given bed depth, in a clogged filter to that in a clean filter
r = ratio of available cross-sectional area at a given bed depth in a filter in its clogged state to that in its clean state
R_h = mean hydraulic radius, cm
t = time, s
t_m = time required for concentration peak arrival at a given bed depth z or at a given axial distance, x, s
$t_{m,e}$ = time required for concentration peak arrival at a given axial distance x based on equivalent system, s
u = interstitial velocity at given bed depth, cm/s
u_s = superficial velocity, based on empty tube cross-sectional area, cm/s
x = axial distance, cm
$\bar{x}$ = axial distance in equivalent system, cm
z = bed depth, cm

Greek Letters

α_k = parameter defined in Equation (27)
β_k = parameter defined in Equations (28) and (29)
$\tilde{\beta}_k$ = parameter defined in Equation (34)
γ_k = parameter defined in Equations (30) and (31)
$\tilde{\gamma}_k$ = parameter defined in Equation (35)
δ_k = parameter defined in Equations (32) and (33)
ϵ = bed voidage
ϵ_d = porosity of particle deposit
λ = ratio of equivalent grain diameter in clogged filter to that in a clean filter
ρ = density of fluid, g/cm^3
σ = specific deposit, volume of deposited matter per unit bed volume
σ_a = apparent specific deposit, volume occupied by deposit per unit bed volume
σ^2 = dimensionless variance of concentration vs. time response, normalized with time constant (z/u_o)
σ_t^2 = variance of concentration vs. time response, s^2
$\Delta\sigma^2$ = difference in the dimensionless variance of concentration vs. time response at two measuring points
$\Delta\sigma_t^2$ = difference in the variance of concentration vs. time response at two measuring points

LITERATURE CITED

Bird, R. B., W. E. Stewart, and E. N. Lightfoot, *Transport Phenomena*, Wiley, New York (1960).
Bischoff, K. B., Ph.D. dissertation, Ill. Inst. Technol., Chicago (1961).
———, and O. Levenspiel, "Fluid Dispersion-generalization and Comparison of Mathematical Models—I: Generalization of Models," *Chem. Eng. Sci.*, **17**, 245-255 (1962).
Camp, T. R., "Theory of Water Filtration," *ASCE Proc. J. San. Eng. Div.*, **90**, No. SA4, 1 (1964).
Cleasby, J. L., and E. R. Baumann, "Selection of Optimum Filtration Rates for Sand Filters," Bulletin 198 of the Iowa Engrg. Expt. Station, *The Iowa State University Bulletin*, Vol. 1X, No. 34 (1962).
Deb, A. K., "Theory of Sand Filtration," *ASCE Proc. J. San. Eng. Div.*, **95**, 399 (1969).
Heertjes, P. M., "Studies in Filtration: Blocking Filtration," *Chem. Eng. Sci.*, **6**, 190 (1957).
Herzig, J. P., J. M. Leclere, and P. LeGoff, "Flow of Suspensions Through Porous Media-Application to Deep Filtration," *Ind. Eng. Chem.*, **62**, No. 5, 8 (1970).
Ison, C. R., and K. J. Ives, "Removal Mechanisms in Deep Bed Filtration," *ibid.*, **24**, 717 (1969).
Ives, K. J., "Rational Design of Filters," *Proc. Inst. Civil Engrs. (London)*, **16**, 189 (1960).
———, Seminar Lectures at the Department of Chemical Engineering and Materials Science, Syracuse Univ., New York (May 20 to 24, 1972).
———, discussion of "Determining Specific Deposit by Backwash Technique," by Kou-ying Hsiung, *ASCE J. Environ. Eng.*, **100**, 1297 (1974).
Leers, R., "Die Abscheiclung Von Schwebstoffen in Faserfiltern," *Staub.*, **50**, 402 (1957).
Maroudas, A., and P. Eisenklam, "Classification of Suspensions: A Study of Particle deposition in Granular Media," *ibid.*, **20**, 867 (1965); **20**, 888 (1965).
Mehter, A. A., R. M. Turian, and Chi Tien, "Filtration in Deep Beds of Granular Activated Carbon," *Res. Rept. 70-3*, FWPCA, Grant No. 17020 DZO, Syracuse Univ., N.Y. (1970).
Mints, D. M., and V. Z. Meltser, "Hydraulic Resistance of a Granular Porous Mass in the Process of Clogging," *Dokl. Akad. Nauk. SSR*, **192**, 304 (1970).
Payatakes, A. C., and Chi Tien, "Applications of the P-T-T

Porous Media Model in Deep Bed Filtration," Particulate Matter Systems Conf., New Henniker, N.H. (August, 1974).
———, and R. M. Turian, "Trajectory Calculation of Particle Deposition in Deep Bed Filtration: I. Model Formulation," *AIChE J.*, **20**, 889 (1974*a*).
———, "II. Case Study of the Effect of the Dimensionless Groups and Comparison with Experimental Data," *ibid.*, 900 (1974*b*).
Payatakes, A. C., D. H. Brown, and Chi Tien, "On the Transient Behavior of Deep Bed Filtration," Paper No. 40 (6), 83rd National Meeting, AIChE, Houston, Tex. (Mar., 1977).
Pendse, Hemant, "Dispersion Measurement in a Clogged Filter," M.S. thesis, Syracuse Univ., N.Y. (1977).
Rajagopalan, R., and Chi Tien, "Trajectory Analysis of Deep Bed Filtration with the Sphere-in-cell Porous Media Model," *AIChE J.*, **22**, 523 (1976).
Stein, P. C., "A Study of the Theory of Rapid Filtration of Water through Sand," D.Sc. dissertation, Mass. Inst. Technol., Cambridge (1940).
Tien, Chi, C. S. Wang, and D. T. Barot, "Chainlike Formation of Particle Deposits in Fluid Particle Separation," *Science*, **196**, 983 (1977).
Yao, K. M., "Influence of Suspended Particle Size on Transport Aspect of Water Filtration," Ph.D. dissertation, Univ. N. C., Chapel Hill (1968).
———, M. T. Habibian, and C. R. O'Melia, "Water and Waste Water Filtration: Concepts and Applications," *Environ. Sci. Tech.*, **5**, 1105 (1971).

Manuscript received July 19, 1977; revision received December 23, 1977, and accepted January 5, 1978.

Inferential Control of Processes:

BABU JOSEPH
and
COLEMAN B. BROSILOW
Case Institute of Technology
Case Western Reserve University
Cleveland, Ohio 44106

Part I. Steady State Analysis and Design

Methods are presented for the design of a static estimator which infers unmeasurable product qualities from secondary measurements. The secondary measurements are selected so as to minimize the number of such measurements required to obtain an accurate estimate which is insensitive to modeling errors. Unlike previous work, the number of secondary measurements can be fewer than the number of unmeasured disturbances. If the statistics of the disturbances and/or measurement noise are available, this information can be incorporated into the design procedure to obtain an optimal static estimator.

The design procedure is illustrated by application to a simulated industrial debutanizer. Data for the simulation were supplied by the Marathon Oil Company. Deviations in bottoms product quality are compared for the current control policy (maintenance of a stage temperature at its set point) and the inferential control system with the column subjected to representative feed composition disturbances. Results show that inferential control based on four, five, or six tray temperature measurements improves the steady state control performance by as much as 400%.

SCOPE

An inferential control system uses measurements of secondary process outputs, such as temperatures, to infer the effect of unmeasurable disturbances on primary process outputs, such as product quality. The control system uses its inference to adjust the control effort to counteract the effect of the unmeasurable disturbances on the product quality. Inferential control can be viewed as an extension of feedforward control which infers the effect of measurable disturbances on the product quality and adjusts the control effort to counteract the effect of the measured disturbances. Feedforward and inferential control can be applied simultaneously.

These three papers present a strategy for the design of linear inferential control systems for processes which operate about a sequence of steady states. The unmeasurable disturbances are assumed to drift from one mean level to another at a rate such that the process will operate about one or another steady state condition most of the time. The above assumption is, of course, motivated by our picture of the operation of most chemical and petroleum process.

Babu Joseph is at the Massachusetts Institute of Technology, Cambridge, Massachusetts.